Article ID: 1000-324X(2020)03-0301-08 **DOI:** 10.15541/jim20190350

Adsorption of Cr(VI) from Aqueous Solution by Biochar-clay Derived from Clay and Peanut Shell

WANG Hai, YANG Ningcan, QIU Muqing

(School of Life Science, Shaoxing University, Shaoxing 312000, China)

Abstract: Heavy metal chromium pollution seriously threatens the environmental safety of soil and water body. The Cr(VI) compound has strong migration ability, enrichment and strong oxidizing ability. These properties make Cr(VI) ions more dangerous and difficult to handle. Adsorption technology is a simple and effective method for treatment of heavy metal pollution. The two clay-biochars are made by mixing biochar derived from peanut shell and two kinds of clays (Kaolin and bentonite) under magnetic stirring conditions. A variety of characterizations suggest that clays uniformly deposit on the surface of biochar. Adsorption experiments indicate that the sorption of Cr(VI) ions from wastewater on Kaolin-biochar is significantly higher than that of bentonite-biochar. Adsorption kinetic of Cr (VI) on two clay-biochars follows satisfactorily the pseudo-second order model due to high correlation coefficient (R^2>0.999). Adsorption isotherms of Cr(VI) on Biochar@Bentonite are fitted by Langmuir model, whereas the Freundlich model fits better the Cr(VI) sorption on Biochar@Kaolin. These findings are crucial for the potential application of clay-biochar composites for the treatment of the immobilization of heavy metals in environmental remediation.

Key words: adsorption; peanut shell; clay-biochar; Cr(VI)

At present, heavy metal chromium pollution mainly comes from metallurgy, leather, dye, mining, electroplating and other industries[1]. It seriously threatens the environmental safety of soil and water body. The chromium in the wastewater emitted into the environment mainly exists in two valence states, Cr(III) ion and Cr(VI) ion[2]. Among them, Cr(III) ions in solution have almost no toxicity. However, Cr(VI) ion is carcinogenic, teratogenic and mutagenic, and highly toxic even at low concentrations[3]. In addition, the Cr(VI) compound has strong migration ability, enrichment and strong oxidizing ability. These properties make Cr(VI) ions more dangerous and difficult to be treated[4-6]. Therefore, research on pollution control of chromium wastewater becomes a hot spot in the control of environmental pollution[7-9].

Adsorption technology is a simple and effective method for treatment of heavy metal pollution[10-11]. Among the adsorbent materials, biochar is a kind of highly aromatic and difficult to capacity solid material formed by waste biomaterials under high temperature thermal cracking under conditions of oxygen deficiency or low oxygen[12-13]. They are mostly composed of loose porous, ordered aromatic rings. They have well-developed pore structure, large specific surface area, dense surface charge and rich in carboxyl, sulfhydryl and phenolic hydroxyl groups[14-16]. As a kind of agricultural and forestry waste, peanut shells are used as fuel, except for a small number of them used to make feed and building materials. This is harmful to the environment, and wastes resources. Based on above advantages, peanut shells are often used to prepare for biochar[17].

In recent years, various natural clay materials have been used in the adsorption research of heavy metal ions due to their low cost and easy reproducibility[18]. The experimental results showed that natural clays, such as bentonite, kaolin and diatomaceous earth, have strong adsorption capacity for heavy metal ions because of their negative charge[19]. However, its adsorption capacity for negatively charged Cr(VI) is relatively weak. Therefore, it is generally necessary to modify the natural clay to

Received date: 2019-07-15; **Revised date:** 2019-09-25
Foundation item: National Natural Science Foundation of China (21876115); Public Welfare Program of Zhejiang Natural Science (LGF19C030001)
Biography: WANG Hai(1981–), male, associate professor. E-mail: wanghai@usx.edu.cn
王 海(1981–), 男, 副教授. E-mail: wanghai@usx.edu.cn
Corresponding author: QIU Muqing, associate professor. E-mail: qiumuqing@126.com
邱木清, 男, 副教授. E-mail: qiumuqing@126.com

adsorb the Cr(VI) in solution[20-22].

The objective of this study is to prepare two clay-biochars and to investigate the effect of water chemical characteristics (*e.g.*, initial solution pH, ionic strength, Cr(VI) concentration and contact time) on Cr(VI) adsorption on two clays-biochars by batch techniques. The highlight of this study is to apply biochar-based composites for decontamination of heavy metals in environmental clean up.

1 Materials and methods

1.1 Materials

Kaolin and bentonite (>99.5% purity) are purchased from Sinopharm Chemical Reagent Co., Ltd. Peanut shell is obtained from vegetable market of Shaoxing city (Zhejiang province, China).

1.2 Preparation of two clay-biochars

Two clay-biochars of peanut shell@Kaolin (Biochar @Kaolin) and peanut shell@Bentonite (Biochar@Bentonite) are obtained by mixing biochar derived peanut shell and two kinds of clays under magnetic stirring conditions. Briefly, the peanut shell is firstly washed and then dried at 60 ℃. The pure peanut shell is milled into powders. The peanut shell powder is filled in ceramic crucibles covered with fitted lid. Ceramic crucibles are put in a muffle furnace and burned under oxygen-limited conditions at 250 ℃ for 2 h. Then the biochar derived from peanut shell is cooled to room temperature. The obtained biochar derived from peanut shell is powdered and passed through a 150 μm(100 mesh) screen.

Then, 30 g biochar, 30 g Kaolin and Bentonite are added to 600 mL deionized water, and reacted for 2 h under vigorous stirring condition. Then, the suspensions are centrifuged at 6000 r/min for 10 min. The Biochar@Kaolin and Biochar@Bentonite are obtained by drying at 105 ℃ overnight and sieved through a 150 μm (100 mesh) screen.

1.3 Adsorption experiments

Adsorption experiments are conducted in 250 mL Erlenmeyer flasks containing the clay-biochar and 100 mL Cr(VI) ion solutions with various initial concentrations. The initial pH is adjusted with HCl or NaOH solution. The flasks are placed in a shaker at a constant temperature and 200 r/min. The samples are filtered and analyzed.

1.4 Characterizations

The morphology of clay-biochar was observed with SEM (JEOL 6500F, Japan) and TEM (JEM-F200, Japan). XRD analysis was conducted in a D/Max-IIIA Powder X-ray Diffractomer (Rigaku Corp., Japan). NOVA 4200e Surface area and Pore size analyzer (Quantachrome, FL, USA) were used to analyze the surface area and pore size of clay-biochar at a relative pressure of 0.95. XPS (X-ray photoelectron spectrometer, Krato AXIS Ultra DLD, Japan) and the model Axis-HS (Kratos Analytical) were used to determine surface composition. FT-IR spectra of the samples were recorded on a Nexus 670 FT-IR spectrometer (Thermo Nicolet, Madison) in the wavenumber range of 400–4000 cm^{-1}.

The concentration of Cr(VI) ion is analyzed by atomic absorption spectrophotometry.

The q_t (mg/g) is calculated as follows:

$$q_t = \frac{(C_0 - C_t) \times V}{m} \quad (1)$$

where C_0 (mg/L) and C_t (mg/L) are the initial and equilibrium liquid-phase concentrations of Cr(VI) ion respectively. V (L) is the solution volume and m (g) is the mass of adsorbent used.

1.5 Statistical analyses of data

All experiments were repeated in duplicate, and the data were analyzed by the mean and standard deviation (SD). The value of the SD was calculated by Excel Software. All error estimates given in the text and error bars in figures were standard deviation of means (mean± SD). All statistical significance was noted at α=0.05 unless otherwise noted.

2 Results and discussion

2.1 Characterization

The surface area and average pore size of Biochar, Biochar@Kaolin and Biochar@Bentonite are listed in Table 1. As listed in Table 1, the BET specific surface area of Biochar@Kaolin and Biochar@Bentonite are 6.15 and 3.08 m^2/g respectively, which is higher than that of biochar (2.79 m^2/g). The total pore volume and the average pore width of Biochar@Kaolin and Biochar@ Bentonite are also higher than that of original Biochar. Clay contains a proportion of mineral element, which have small surface areas and rich transitional pores, and the added clay does not block pore openings of the biochar[23].

The surface characteristics of Biochar@Kaolin and Biochar@Bentonite are shown in Fig. 1 and Fig. 2. As shown in Fig. 1 and Fig. 2, Biochar@Kaolin and

Table 1 Characterizations of Biochar, Biochar@Kaolin and Biochar@Bentonite

Sample	BET specific surface area/($m^2 \cdot g^{-1}$)	Average pore width/nm
Biochar	2.79	39.37
Biochar@Kaolin	6.15	83.41
Biochar@Bentonite	3.08	56.18

Biochar@Bentonite have rough surface with some fine particles, which indicate that the Kaolin and Bentonite successfully load on the Biochar.

EDS spectra of the Biochar@Kaolin and Biochar@Bentonite before and after the reaction with Cr(VI) are shown in Fig. 3. Biochar@Kaolin and Biochar@Bentonite contain substantial amounts of C, O Si and Al as well as a few of Ca, Na, Fe and K, which are typical of the elemental composition of clay minerals. The presence of Cr(VI) after adsorption experiment indicates that Cr(VI) is effectively removed by Biochar@Kaolin and Biochar@Bentonite[23]. XRD patterns of Biochar@Kaolin and Biochar@Bentonite samples are shown in Fig. 4. The characteristic peaks at 2θ=20.64° and 26.40° are identified as (*hkl*) and (*hkl*) plane of expansible phyllosilicates respectively. XRD analysis suggests that the Kaolin and Bentonite successfully load on the surfaces of biochar, which are consistent with the EDS results[24].

FT-IR spectra are used to determine the surface functional groups. FT-IR spectra of Biochar, Kaolin, Bentonite, Biochar@Kaolin and Biochar@Bentonite are depicted in Fig. 5.

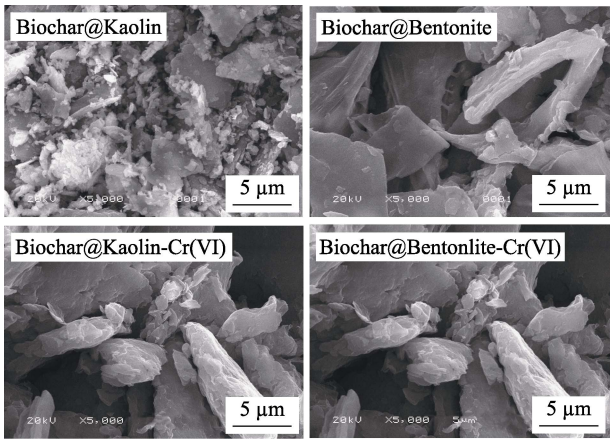

Fig. 1　SEM images of the Biochar@Kaolin and Biochar@Bentonite before and after the reaction with Cr(VI)

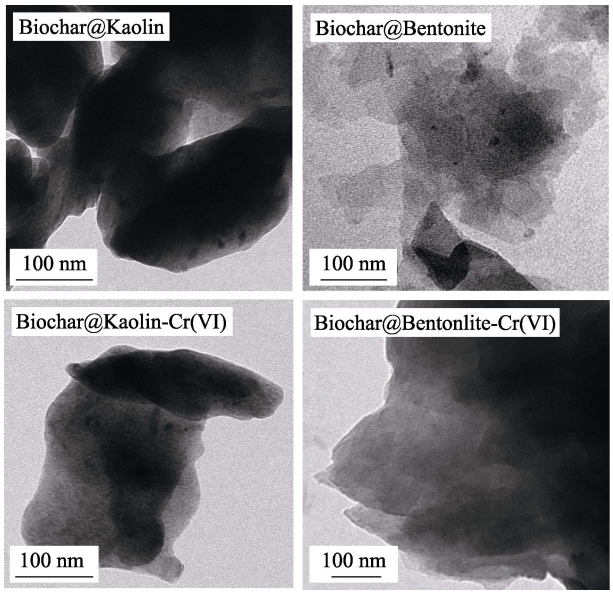

Fig. 2　TEM images of the Biochar@Kaolin and Biochar@Bentonite before and after the reaction with Cr(VI)

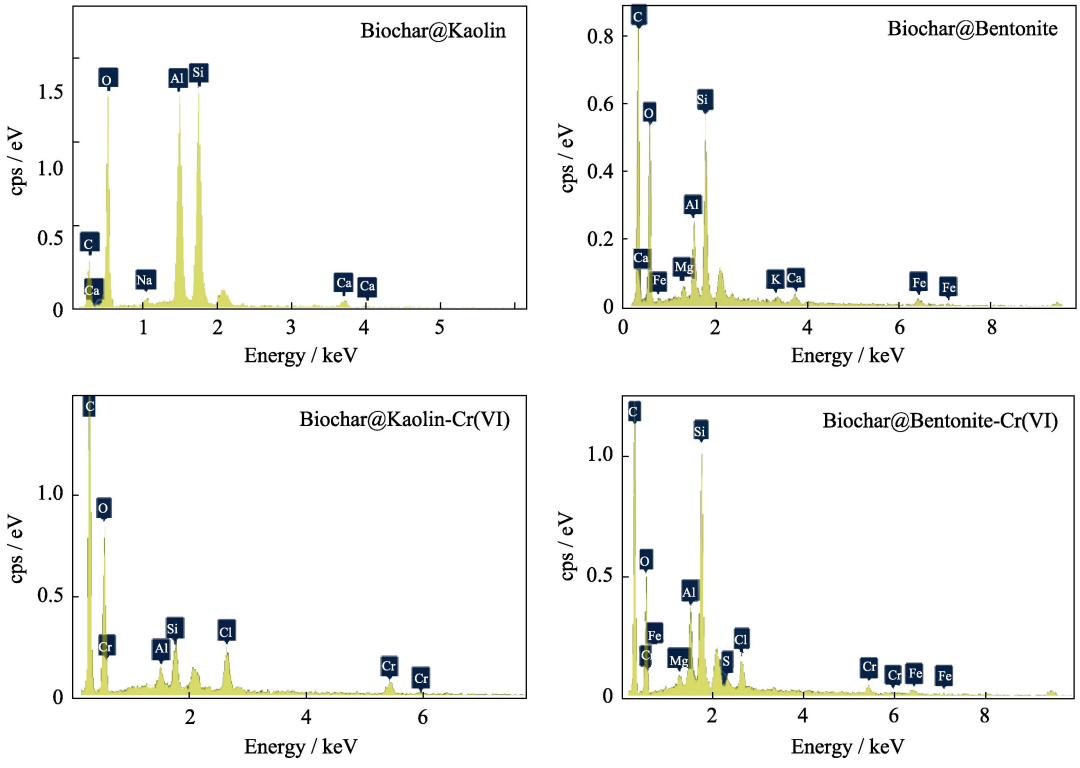

Fig. 3　EDS spectra of the Biochar@Kaolin and Biochar@Bentonite before and after the reaction with Cr(VI)

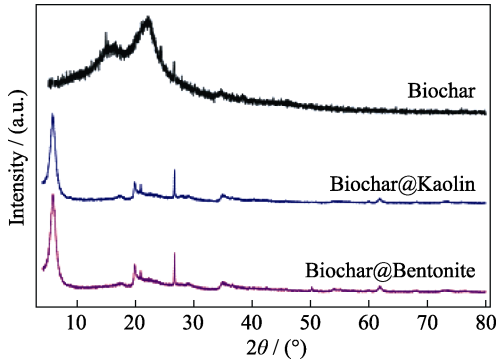

Fig. 4 XRD patterns of Biochar, Biochar@Kaolin and Biochar@Bentonite

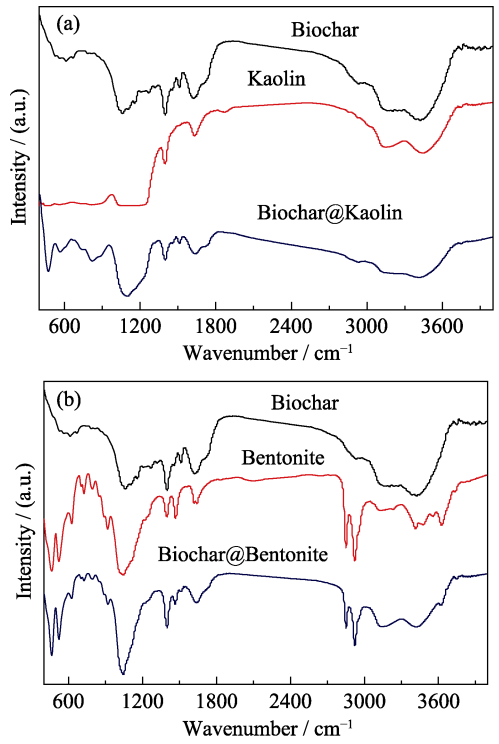

Fig. 5 FT-IR spectra of Biochar, Kaolin, Bentonite, Biochar@Kaolin and Biochar@Bentonite

As shown in Fig. 5, the peaks of Biochar@Kaolin and Biochar@Bentonite at approximately 3420, 1400, 1020–1100 and 520–460 cm^{-1} are assigned to the stretching vibration of the –OH, COO–, –C–O and –C–OH or Si–O group, respectively[25]. The surface of compositions and chemical states of clay-biochar are further investigated by XPS. The C1s XPS spectra of Biochar@Kaolin and Biochar@Bentonite are shown in Fig. 6.

The C1s XPS spectra of Biochar@Kaolin and Biochar@Bentonite is the major component with peaks at 284.4 eV, which may be assigned to C/N–O, C–O or C–C bonds[26]. These results suggest that Biochar@Kaolin and Biochar@Bentonite contain considerable amounts of oxygen/nitrogen groups on its surface, which is beneficial for binding Cr(VI) ions[21].

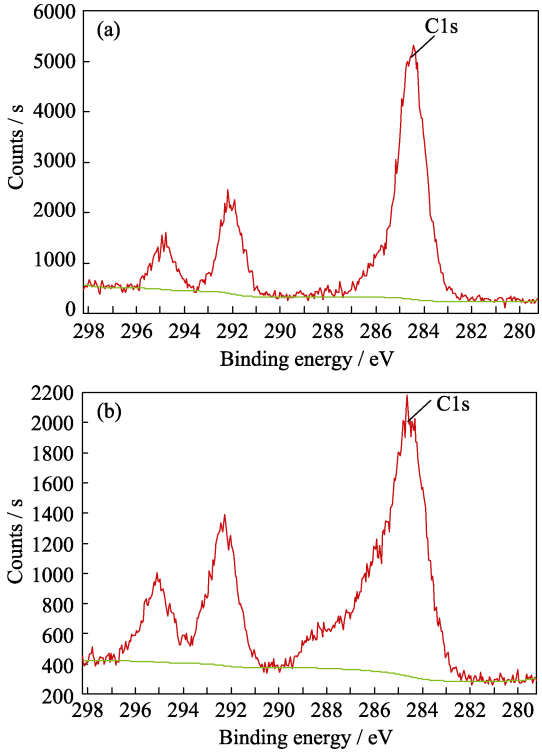

Fig. 6 XPS spectra of Biochar@Kaolin (a) and Biochar@Bentonite (b)

2.2 Effect of pH

The Cr(VI) removal efficiencies and adsorption capacities of Biochar@Kaolin and Biochar@Bentonite in solution with pH of 1–14 are shown in Fig. 7. As shown in Fig. 7, pH plays an important role in the removal of Cr(VI) in aqueous solution. At pH<7, the removal rate of Cr(VI) ions increase with pH decreasing. Under the acidic solution, the surface of Biochar@Kaolin and Biochar@Bentonite is positively charged, and is beneficial for the adsorption of Cr(VI) ion by electrostatic attraction[25]. At pH>7, the removal rate of Cr(VI) ions increases with pH increasing due to the precipitation of Cr(VI). Previous studies have also shown that precipitation could play an important role in controlling the removal of heavy metal ions from aqueous solution by biochars at high pH[26].

2.3 Effect of SO_4^{2-} ion in solution

The effect of SO_4^{2-} ion on the removal of Cr(VI) by the Biochar@Kaolin and Biochar@Bentonite is shown in Fig. 8. No effect of SO_4^{2-} on the removal of Cr(VI) ions by Biochar@Kaolin, whereas the removal rates of Cr(VI) on Biochar@Bentonite decreased with the increase of SO_4^{2-} ions concentration. These may be attributed to the fact that there are much Na^+ and Ca^{2+} ions exit on the surface of Biochar@Bentonite, but none of charged ions on the surface of Biochar@Kaolin. For specific adsorption sites, Cr(VI) ions are preferentially adsorbed over the SO_4^{2-} ions. When the specific adsorption sites are

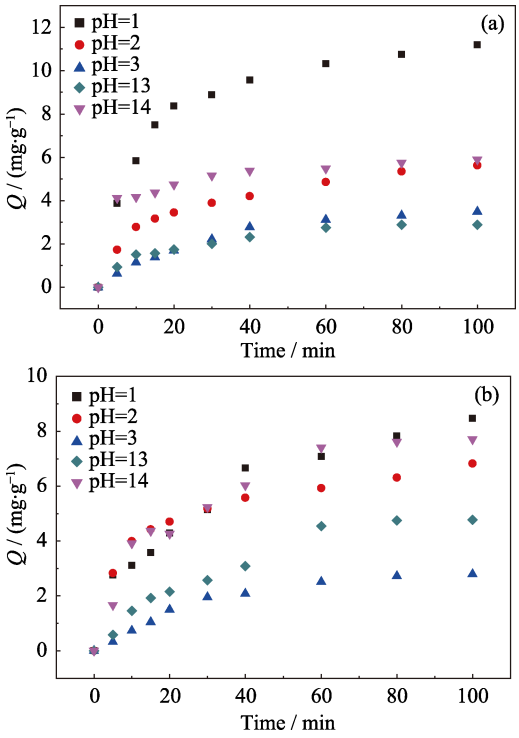

Fig. 7　Effect of pH on the removal of Cr (VI) by the Biochar@Kaolin (a) and Biochar@Bentonite (b)

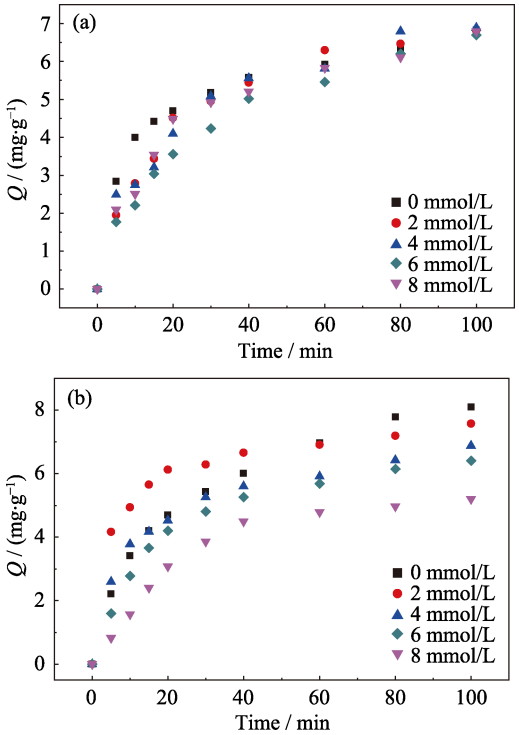

Fig. 8　Effect of SO_4^{2-} on the removal of Cr (VI) by the Biochar@Kaolin (a) and Biochar@Bentonite (b)

saturated, the exchange reactions of dominate and competition for these sites between Cr(VI) ions and SO_4^{2-} ions are important[27-28].

2.4　Sorption kinetics

Fig. 9(a) shows the adsorption data of Cr(VI) on different kinds of adsorbents. The sorption shows a rapid initial uptake followed by smooth increase. Kinetics studies are carried out and a number of well-known sorption models are applied in order to better understand the processes governing the adsorption of Cr(VI) ions to the Biochar@Kaolin and Biochar@Bentonite[29].

In this study, the pseudo-first order and pseudo-second order kinetic models are used to predict the kinetic data. The pseudo-second order rate law bases on the assumption that the rate of solute sorption is directly proportional to the square of the number of vacant binding sites. The pseudo-first order and pseudo-second order[30-31] are described as Eq. (2) and (3):

$$\frac{dq_t}{dt} = k_1(q_e - q_t) \tag{2}$$

$$\frac{dq_t}{dt} = k_2(q_e - q_t)^2 \tag{3}$$

Where q_e (mg/g) is the amount of adsorbed solute at equilibrium conditions, q_t (mg/g) is the amount of adsorbed solute at the time t (min), k_2 (min^{-1}) and k_1 (min^{-1}) are the constants of pseudo-second order and pseudo-first order kinetic model respectively.

The plots of two models for Cr(VI) ions adsorbed onto the biochar, Biochar@Kaolin and Biochar@Bentonite are shown in Fig. 9. The corresponding calculated parameters are listed in Table 2.

The sorption kinetics of Cr(VI) on biochar, Biochar@Kaolin and Biochar@Bentonite are satisfactorily fitted by pseudo-second order model due to the higher correlation coefficient value (R^2 >0.98). It indicates that the chemisorption is involved in covalent interaction due to the sharing and exchange of electrons between Cr(VI) ions, and the adsorbent is likely the primary rate-limiting step involved in Cr(VI) ions sorption on surfaces of adsorbent[32-34].

2.5　Sorption isotherms

Langmuir isotherm model describes the correlation between the amounts of solute adsorbed on adsorbent (mg/g) *versus* the solute concentration in the solution (mg/L) at equilibrium condition. This model assumes that at equilibrium, monolayer sorption of solute occurs at fixed number of homogeneously distributed sorption sites over the adsorbent surface, and these sites also have equal affinity for the adsorbate. The non-linear equations describing the Langmuir isotherm model is given as follows[35-36]:

$$q_e = \frac{Q_{max} K_L C_e}{1 + K_L C_e} \tag{4}$$

Where C_e (mg/g) is the solute aqueous concentration at equilibrium, q_e (mg/g) is the amount of solute adsorbed per unit weight of adsorbent at equilibrium, Q_{max} is the

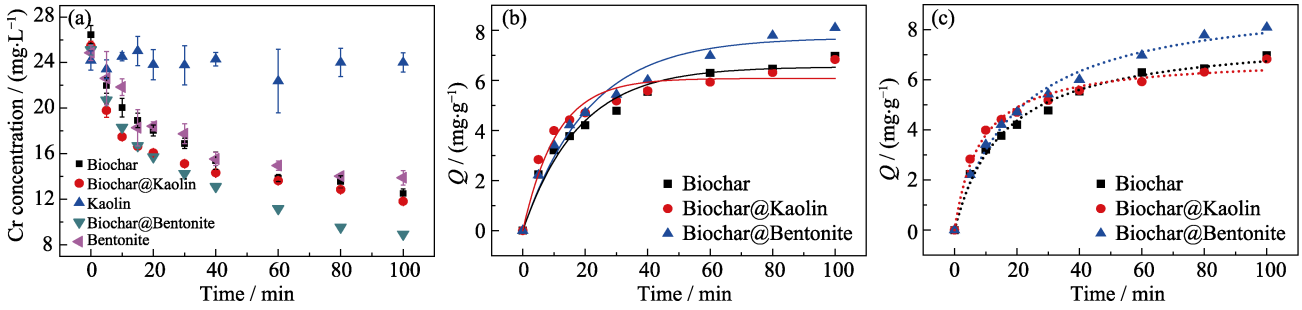

Fig. 9 Adsorption data and modeling for Cr(VI) ions removal by Biochar, Biochar@Kaolin and Biochar@Bentonite, respectively
(a) Adsorption data; (b) Pseudo-first order kinetic; (c) Pseudo- second order

Table 2 Pseudo-first order kinetic and pseudo-second order kinetic parameters of Cr(VI) ions removal by Biochar, Biochar@Kaolin and Biochar@Bentonite

Sample	Pseudo-first-order			Pseudo-second-order		
	q_e/(mg·g^{-1})	k_1/min^{-1}	R^2	q_e/(mg·g^{-1})	K_2/(g·mg^{-1}·min^{-1})	R^2
Biochar	6.54	0.056	0.967	7.80	0.063	0.990
Biochar@Kaolin	7.07	0.092	0.947	8.91	0.122	0.986
Biochar@Bentonite	7.70	0.048	0.971	9.41	0.052	0.991

maximum amount of solute adsorbed per unit weight of adsorbent (mg/g) to form a single layer, and K_L (L/mg) is the isotherm constant.

The Freundlich isotherm model assumes that the sorption process on a heterogeneous surface is in the form of multilayers, where adsorption sites have varied affinity for the adsorbate. The non-linear forms of the Freundlich isotherm model can be presented as[37-38]:

$$q_e = K_F C_e^{1/n} \quad (5)$$

Where C_e (mg/g) is the solute aqueous concentration at equilibrium, q_e (mg/g) is the amount of solute adsorbed per unit weight of adsorbent at equilibrium, K_F ((mg/g)$^{1/n}$) and $1/n$ are the isotherm constants.

According to experimental data, the adsorption isotherms parameters of Cr(VI) ion removal by biochar, Biochar@Kaolin and Biochar@Bentonite at different temperatures can be calculated and listed in Table 3.

According to the value of R^2, the simulations of the Langmuir model fits the adsorption data well and can therefore be used to describe the Cr(VI) ions adsorption behavior at different temperatures for Biochar@Bentonite. It also indicates that the adsorption process is homogeneous adsorption. The Cr(VI) ion from aqueous solution adsorption on the Biochar@Bentonite is monolayer adsorption. The maximum adsorption capacities of Biochar@Bentonite are calculated to be 20.54, 23.64 and 27.23 mg/g at 20, 30 and 40 ℃, respectively. For Biochar@Kaolin, the Freundlich adsorption model shows a better fit to the sorption data at different temperatures. It is also suggested that the sorption process on a heterogeneous surface is in the form of multilayers adsorption.

3 Conclusions

Two clay-biochars were successfully developed in this study. The batch experiments indicate that clay-biochar composite has high adsorption ability to Cr(VI) ion from aqueous solution (20.54, 23.64 and 27.23 mg/g at 20, 30 and 40 ℃, respectively). The adsorption kinetics

Table 3 Parameters of adsorption isotherms for Cr(VI) ions removal by Biochar, Biochar@Kaolin and Biochar@Bentonite at 20, 30 and 40 ℃, respectively

T/℃	Sample	Langmuir adsorption model			Freundlich adsorption model		
		Q_{max}/(mg·g^{-1})	K_L/(L·mg^{-1})	R^2	K_F/((mg·g)$^{-1/n}$)	$1/n$	R^2
20	Biochar@Kaolin	15.58	0.0029	0.978	3.57	0.0064	0.995
	Biochar@Bentonite	20.54	0.035	0.980	6.75	0.0042	0.903
30	Biochar@Kaolin	68.98	0.0063	0.940	4.55	0.0083	0.992
	Biochar@Bentonite	23.64	0.058	0.967	10.53	0.0033	0.942
40	Biochar@Kaolin	76.62	0.13	0.795	9.61	0.0028	0.996
	Biochar@Bentonite	27.23	0.28	0.956	14.82	0.0016	0.852

can be satisfactorily fitted by pseudo-second order model. The adsorption isotherms of Cr(VI) on Biochar@Bentonite can be fitted by Langmuir model, whereas the Freundlich model fits better the Cr(VI) sorption on Biochar@Kaolin at different temperatures. These observations indicate that biochar-based composites can be regarded as the promising adsorbents for immobilization of heavy metals in environmental cleanup.

References:

[1] ALEKSANDRA B, PATRYK O, RYSZARD D. Application of laboratory prepared and commercially available biochars to adsorption of cadmium, copper and zinc ions from water. *Biores. Technol.*, 2015, **196:** 540–549.

[2] JIANG S S, HUANG L B, TUAN A H, *et al.* Copper and zinc adsorption by softwood and hardwood biochars under elevated sulphate-induced salinity and acidic pH conditions. *Chemosphere*, 2016, **142:** 64–71.

[3] LYU H, TANG J, HUANG Y, *et al.* Removal of hexavalent chromium from aqueous solutions by a novel biochar supported nanoscale iron sulfide composite. *Chem. Eng. J.*, 2017, **322:** 516–524.

[4] PAN J J, JIANG J, XU R K, Removal of Cr(VI) from aqueous solutions by Na_2SO_3/$FeSO_4$ combined with peanut straw biochar. *Chemosphere*, 2014, **101:** 71–76.

[5] ZHU K R, CHEN C L, LU S H, *et al.* MOFs-induced encapsulation of ultrafine Ni nanoparticles into 3D N-doped grapheme-CNT frameworks as a recyclable catalyst for Cr(VI) reduction with formic acid. *Carbon*, 2019, **148:** 52–63.

[6] WEN T, WANG J, YU S J, *et al.* Magnetic porous carbonaceous material produced from tea waste for efficient removal of As(V), Cr(VI), humic acid and dyes. *ACS Sustainable Chem. Eng.*, 2017, **5:** 4371–4380.

[7] GAO Y, CHEN C L, TAN X L, *et al.*, Polyaniline-modified 3D-flower-like molybdenum disulfide composite for efficient adsorption/photocatalytic reduction of Cr(VI). *J. Colloid Interf. Sci.*, 2016, **476:** 62–70.

[8] HU B W, HU Q Y, XU D, *et al.* The adsorption of U(VI) on carbonaceous nanofibers: a combined batch, EXAFS and modeling techniques. *Sep. Pur. Technol.*, 2017, **175:** 140–146.

[9] ZHU K R, CHEN C L, XU H, *et al.* Cr(VI) reduction and immobilization by core-double-shell structured magnetic polydopamine@ zeolitic ldazolate framevorks-8 microspheres. *ACS Sustainable Chem. Eng*., 2017, **5:** 6795–6802.

[10] WEN T, WANG J, LI X, *et al.* Production of a generic magnetic Fe_3O_4 nanoparticles decorated tea waste composites for highly efficient sorption of Cu(II) and Zn(II). *J. Environ. Chem. Eng.*, 2017, **5:** 3656–3666.

[11] HU B W, QIU M Q, HU Q Y, *et al.* Decontamination of Sr(II) on magnetic polyaniline/graphene oxide composites: evidence from experimental, spectroscopic, and modeling investigation. *ACS Sustain. Chem. & Eng*., 2017, **5:** 6924–6931.

[12] QIU M Q, WANG M, ZHAO Q Z, *et al.* XANES and EXAFS investigation of uranium incorporation on nZVI in the presence of phosphate. *Chemosphere*, 2018, **201:** 764–771.

[13] HU B W, GUO X J, ZHENG C, *et al.* Plasma-enhanced amidoxime/ magnetic graphene oxide for efficient enrichment of U(VI) investigated by EXAFS and modeling techniques. *Chem. Eng. J.*, 2019, **357:** 66–74.

[14] WANG S, GAO B, ZIMMERMAN A R, *et al.* Removal of arsenic by magnetic biochar prepared from pinewood and natural hematite. *Bioresour. Technol.*, 2015, **175:** 391–395.

[15] GU P C, SONG S, ZHANG S, *et al.* Enrichment of U(VI) on polyaniline modified MXene composites studied by batch experiment and mechanism investigation. *Acta Chim. Sinica*, 2018, **76:** 701–708.

[16] HU B W, CHEN G H, JIN C G, *et al.* Macroscopic and spectroscopic studies of the enhanced scavenging of Cr(VI) and Se(VI) from water by titanate nanotube anchorednanoscale zero-valent iron. *J. Hazard. Mater.*, 2017, **336:** 214–221.

[17] SUN B, CHAI J L, CHAI Z Q, *et al.* A surfactant-free microemulsion consisting of water, ethanol, and dichloromethane and its template effect for silica synthesis. *J. Colloid Interf. Sci.*, 2018, **526:** 9–17.

[18] LI L, HUANG S Y, WEN T, *et al.* Fabrication of carboxyl and amino functionalized carbonaceous microspheres and their enhanced adsorption behaviors of U(VI). *J. Colloid Interf. Sci.*, 2019, **543:** 225–236.

[19] WANG H, GAO B, WANG S, *et al.* Removal of Pb(II), Cu(II), and Cd(II) from aqueous solutions by biochar derived from $KMnO_4$ treated hickory wood. *Bioresour. Technol.*, 2015, **197:** 356–362.

[20] ZHU X, TSANG D C, CHEN F, *et al.* Ciprofloxacin adsorption on graphene and granular activated carbon: kinetics, isotherms, and effects of solution chemistry. *J. Environ. Technol.*, 2015, **36:** 3094–3102.

[21] SHI S Q, YANG J K, LIANG S, *et al.* Enhanced Cr(VI) removal from acidic solutions using biochar modified by Fe_3O_4@SiO_2-NH_2 particles. *Sci. Total Environ.*, 2018, **628-629:** 499–508.

[22] YAO Y, GAO B, FANG J, *et al.* Characterization and environmental applications of clay-biochar composites. *Chem. Eng. J.*, 2014, **242:** 136–143.

[23] CHEN T, ZHOU Z, XU S, *et al.* Adsorption behavior comparison of trivalent and hexavalent chromium on biochar derived from municipal sludge. *Bioresour. Technol.*, 2015, **190:** 388–394.

[24] ZHU K R, GAO Y, TAN X L, *et al.* Polyaniline-modified Mg/Al layered double hydroxide composites and their application in efficient removal of Cr(VI). *ACS Sustainable Chem. Eng.*, 2016, **4:** 4361–4369.

[25] DONG H, DENG J, XIE Y, *et al.* Stabilization of nanoscale zero-valent iron (nZVI) with modified biochar for Cr(VI) removal from aqueous solution. *J. Hazard Mater.*, 2017, **332:** 79–86.

[26] ZHANG L, FU F L, TANG B. Adsorption and redox conversion behaviors of Cr(VI) on goethite/carbon microspheres and akaganeite/carbon microspheres composites. *Chem. Eng. J.*, 2019, **356:** 151–160.

[27] LIU W, SUN W L, HAN Y F, *et al.* Adsorption of Cu(II) and Cd(II) on titanate nanomaterials synthesized *via* hydrothermal method under different NaOH concentrations: role of sodium content, Colloids Surf, A-physicochem. *Eng. Asp.*, 2014, **452:** 138–147.

[28] PAN J J, JIANG J, XU R K. Adsorption of Cr(III) from acidic solutions by crop straw derived biochars. *J. Environ. Sci.*, 2013, **25:** 1957–1965.

[29] XIAO R, WANG J J, LI R H, *et al.* Enhanced sorption of hexavalent chromium [Cr(VI)] from aqueous solutions by diluted sulfuric acid-assisted MgO-coated biochar composite. *Chemosphere*, 2018, **208:** 408–416.

[30] CHOUDHARY B, PAUL D. Isotherms, kinetics and thermodynamics of hexavalent chromium removal using biochar. *J. Environ. Chem. Eng.*, 2018, **6:** 2335–2343.

[31] REGUYAL F, SARMAH A K, GAO W. Synthesis of magnetic biochar from pine sawdust *via* oxidative hydrolysis of $FeCl_2$ for the removal sulfamethoxazole from aqueous solution. *J. Hazard Mater.*, 2017, **321:** 868–878.

[32] GAN C, LIU Y, TAN X, *et al.* Effect of porous zincebiochar nanocomposites on Cr(VI) adsorption from aqueous solution. *RSC Adv.*, 2015, **5:** 35107–35115.
[33] ALMEIDA C, DEBACHER N, DOWNS A, *et al.* Removal of methylene blue from colored effluents by adsorption on montmorillonite clay. *J. Colloid Interf. Sci.*, 2009, **332:** 46–53.
[34] LANGMUIR I. The adsorption of gases on plane surfaces of glass, mica and platinum. *J. Am. Chem. Soc.*, 1918, **40:** 1361–1403.
[35] ZHANG B G, WANG S, DIAO M H, *et al.* Microbial community responses to vanadium distributions in mining geological environments and bioremediation. *J. Geophys. Res. Biogeo.*, 2019, **124:** 601–615.
[36] INYANG M, GAO B, YAO Y, *et al.* Removal of heavy metals from aqueous solution by biochars derived from anaerobically digested biomass. *Bioresour. Technol.*, 2012, **110:** 50–56.
[37] SHI J X, ZHANG B G, QIU R, *et al.* Microbial chromate reduction coupled to anaerobic oxidation of elemental sulfur or zerovalent iron. *Environ. Sci. Technol.*, 2019, **53:** 3198–3207.
[38] ZHANG B G, CHENG Y T, SHI J X, *et al.* Insights into interactions between vanadium (V) bio-reduction and pentachlorophenol dechlorination in synthetic groundwater. *Chem. Eng. J.*, 2019, **375:** 121965.

花生壳生物炭–黏土吸附水中的 Cr(VI)

王 海, 阳柠灿, 邱木清

(绍兴文理学院 生命科学学院, 绍兴 312000)

摘 要: 重金属铬的污染会严重威胁到土壤和水体的环境安全, 而水中的六价铬化合物则具有很强的迁移性、富集性和氧化性等特性, 更具有危害性且难以处理。吸附法是一种能简单、高效地处理含重金属污水的处理技术。在磁力搅拌条件下采用花生壳生物炭分别与高岭土和膨润土混合制备而成两种生物炭–黏土材料, 并分别对这两种生物炭–黏土的表面特性进行表征。结果发现所选用的两种黏土均能不规则地负载在生物炭的表面。吸附实验结果显示, 生物炭–高岭土(Biochar@Kaolin)吸附铬(VI)的能力显著高于生物炭–膨润土(Biochar@Bentonite)。从吸附动力学方程的分析可以看出, 合成的两种生物炭负载黏土吸附水中的铬(VI)均符合伪二级动力学方程。从吸附等温线分析中可以得到, Biochar@Bentonite 吸附铬(VI)的过程符合 Langmuir 模型, 而 Biochar@Kaolin 吸附铬(VI)的过程符合 Freundlich 模型。研究结果显示, 采用生物炭–黏土的复合材料修复环境中的重金属污染具有广阔的应用前景。

关 键 词: 吸附; 花生壳; 黏土–生物炭; 铬(VI)

中图分类号: TQ174 **文献标识码:** A